

AD-A192 243

THE EFFECTS OF THIN COMPRESSIVE FILMS ON INDENTATION  
FRACTURE TOUGHNESS M. (U) ROCKWELL INTERNATIONAL  
THOUSAND OAKS CA SCIENCE CENTER P H KOBRIN ET AL.

1/1

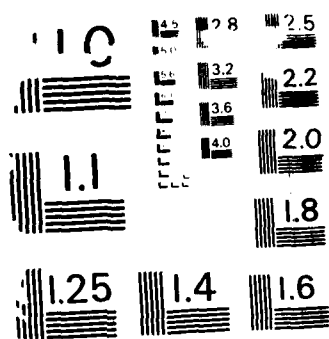
UNCLASSIFIED

N00014-85-C-0140

F/G 11/3

NL





RESOLUTION TEST CHART  
NATIONAL BUREAU OF STANDARDS - 1963-A

AD-A192 243

4

DTIC FILE

THE EFFECTS OF THIN COMPRESSIVE FILMS ON INDENTATION  
FRACTURE TOUGHNESS MEASUREMENTS

P.H. Kobrin and A.B. Harker

Rockwell International Science Center

Thousand Oaks, CA 91360

DTIC  
ELECTE  
MAR 21 1988  
S D  
H

1988  
N00014-85-C-0140

Abstract

Thin compressive films have been shown to decrease the lengths of radial cracks produced by a Vickers indentation in a variety of nonmetallic materials. The intrinsic stress of submicron thick films deposited by reactive ion beam sputtering was measured by a cantilever technique. The change in the apparent indentation fracture toughness of the coated material was correlated with film thickness and stress, indentation load, and the nature of the substrate.

INTRODUCTION

The indentation fracture technique is a simple and rapid means of determining the fracture toughness,  $K_{IC}$ , of brittle materials. In this method, a Vickers-shaped diamond indenter of a given load is used to produce radial cracks that can be viewed on the sample surface. The lengths of the cracks can then be directly related to the fracture toughness.<sup>1</sup>

<sup>1</sup>  
J8257A/jbs

DISTRIBUTION STATEMENT A

Approved for public release;  
Distribution Unlimited

88 3 21 001

A thin stressed layer on the surface of a brittle material can significantly modify the lengths of the radial cracks and therefore also the computed value of the toughness. This phenomenon has been observed in ion-implanted materials by several groups.<sup>2-4</sup> Lawn and Fuller<sup>5</sup> have developed a model that relates thin-layer surface stresses to changes in indentation crack dimensions. Their model predicts a change in the computed fracture toughness,  $K$ , that is independent of indenter load. However, work with ion implantation surface layers<sup>3,4</sup> shows that the change in  $K$  is smaller at larger loads than at smaller loads.

In this paper, a systematic study is described in which changes in the indentation fracture toughness of a variety of brittle materials are correlated with thin film stress and thickness, and with indenter load.

## EXPERIMENTAL

Reactive ion beam deposition was used to deposit thin ( $< 1 \mu\text{m}$ )  $\text{Si}_3\text{N}_4$ ,  $\text{SiO}_2$  and  $\text{Al}_2\text{O}_3$  films from elemental and ceramic targets. Depositions were made at room temperature. These sputtered films are intrinsically stressed as depicted in Fig. 1. This figure shows a model of the relaxed stress distribution of a film/substrate system.<sup>6</sup> The compressive stress in the film is balanced by a tensile stress in the bulk which will cause an unclamped substrate to bend. The resultant stress is highest near the film-substrate interface. This stress is intrinsic to the growth conditions and does not develop as a result of a

For	
I	<input checked="" type="checkbox"/>
d	<input type="checkbox"/>
ion	<input type="checkbox"/>

2  
J8257A/jbs



By <i>per Letter</i>	
Distribution/	
Availability Codes	
Dist	Avail and/or Special
A-1	

mismatch in the thermal expansion coefficients of the film and substrate. Furthermore, for amorphous or polycrystalline films it is expected to be independent of the nature of the substrate.

The intrinsic stresses of the films used in this study were measured by a sensitive bending plate technique with capacitive detection.<sup>7</sup> For this technique, a thin glass cover slip is coated on one side with 20 nm of aluminum metal to make it conductive. The cover slip is then clamped at one end so that it forms a parallel plate capacitor with a metal plate. When a stressed film is deposited on the uncoated side of the cover slip, the glass bends and the resulting change in capacitance is used to measure the film stress. Typically, 10 - 50 nanometers of film were deposited; the ion gun was turned off and the capacitive system was allowed to equilibrate thermally before the stress was determined. Additional depositions were made until 500 nm had been deposited.

Corroboration of the cantilever determined stress values was obtained by measuring the stress of a 400 nm thick  $\text{Si}_3\text{N}_4$  film on a thin, round ZnS substrate. Film stress caused the ZnS substrate to assume a spherical curvature that was measured by counting the Newton's rings under a sodium lamp. The seven rings that were measured from a 0.4 micron thick  $\text{Si}_3\text{N}_4$  film corresponded to a film stress of 1.4 GPa. This is reasonably close to the 1.6 GPa value obtained by the cantilever system. The cover-slip cantilever system is coated stationary, while all of the other substrates in this study were mounted on a rotating planetary substrate holder that produced uniform film coverage.

The Vickers indent technique was used to measure the fracture toughness. The fracture toughness,  $K_{IC}$ , in an unstressed material is given by<sup>1</sup>

$$K_C = xP/c_0^{3/2} \quad (1)$$

where  $P$  is the load, and  $c_0$  is the radial crack length defined in Fig. 2. The coefficient  $x$  is defined by  $x = (0.016)(E/H)^{1/2}$ , where  $E$  and  $H$  are the Young's modulus and hardness, respectively. This technique provides a measure of the fracture toughness that is independent of the indenter load. Figure 3a shows a glass sample that has been indented with a 1.0 kg load. The glass slide was broken along two of the cracks to expose the radial cracks lying beneath the surface. The full penny-like (or semicircular) shape of the radial cracks did not develop because of a lateral crack 40  $\mu\text{m}$  below the surface. Note how the radial cracks intersect the surface at right angles.

A film-stressed system can alter the size and shape of the penny-like radial cracks as well as the indenter loading required to produce four symmetrical cracks. This crack alteration produces a different apparent fracture toughness. Figure 3b shows the effect of adding a 0.4  $\mu\text{m}$  thick  $\text{Si}_3\text{N}_4$  film. The radial cracks are deflected near the surface which results in a shorter crack length on the surface. The shapes of the cracks are modified at a depth beneath the surface that is many times the film thickness. Deflected radial cracks were also observed for films on single crystal silicon substrates.

Films up to 1  $\mu\text{m}$  thick were initially grown on 1.2 mm thick soda lime glass (Erie Scientific, New Hampshire) and 0.3 mm thick (100) single crystal silicon substrates. Indents were made at several loadings and crack lengths were measured at least one day later. The delay between indentation and crack analysis was established since cracks in glass may continue to grow after the

load is removed due to moisture assistance. The rate of this postindentation growth decreases with time.<sup>1</sup> Silicon does not exhibit postindentation growth. Measurements made immediately after indentation provide a more accurate  $K_c$  for unstressed materials.<sup>1</sup> The indenter was aligned so that the cracks in silicon were always oriented along the  $\langle 100 \rangle$  directions.  $K$  was calculated for indents with four radial cracks and with  $c \geq 2b$ . This put a lower limit on the loads and the depths that were sampled. The hardness of the samples, which was also obtained from the Vickers indent, was not noticeably changed by the addition of these films.

## RESULTS AND DISCUSSION

The cantilever stress system gives values of  $\sigma_s$  equal to 0.2, 1.0 and 1.6 GPa for films of  $Al_2O_3$ ,  $SiO_2$  and  $Si_3N_4$ , respectively. In all cases the accumulated stress was found to increase linearly with thickness.

While the stress of the  $SiO_2$  films is less than that of the  $Si_3N_4$ , it was observed that on glass the threshold load for crack production was higher with the  $SiO_2$  films. Glass with a 1.0  $\mu m$  thick  $SiO_2$  film required greater than a 1.5 Kg load for any radial cracks to form while uncoated glass gave four cracks with a 0.2 Kg load. Glass with a 0.5  $\mu m$  thick  $Si_3N_4$  film requires a 0.4-0.7 Kg load to crack. Thus, with an  $SiO_2$  film the crack initiation load increased by an order of magnitude. Greater adhesion or better protection against moisture-assisted crack growth in the  $SiO_2$ /glass system than in the  $Si_3N_4$ /glass system may be responsible for the larger threshold load.

As a first approximation to the change in fracture toughness, Lawn and Fuller<sup>5</sup> have derived a thin-film stress intensity factor for a penny-like crack system

$$K_f = 2\gamma\sigma_s d^{1/2} \quad (2)$$

where  $d$  is the film thickness,  $\gamma$  is a crack geometry term taken to be unity, and  $\sigma_s$  is the average surface stress of the film. Implicit in the derivation of Eq. (2) is the assumption that the crack remains penny-like, which is not the case, as is shown in Fig. 3. Lawn and Fuller pointed out that this non penny-like shape will lead to some uncertainty in Eq. (2).

The measured apparent fracture toughness,  $K$ , is given by the sum of the uncoated fracture toughness plus the thin film stress intensity factor:

$$K = xP/c^{3/2} = K_c + K_f = K_c + 2\sigma_s d^{1/2} \quad (3)$$

Using the cantilever stress measurements, calculated  $K_f$  values for 1.0  $\mu\text{m}$  thick films are 3.2, 2.0 and 0.4  $\text{MPam}^{1/2}$  for  $\text{Si}_3\text{N}_4$ ,  $\text{SiO}_2$  and  $\text{Al}_2\text{O}_3$ , respectively. Equation (3) predicts an increased fracture toughness which is independent of load and sampling depth. Equation (3) also predicts that the magnitude of the increased fracture toughness will be independent of the substrate since  $\sigma_s$  in the  $K_f$  term is independent of the substrate. The effect of tensile stress in the substrate may reduce the fracture toughness below that predicted by Eq. (3) and this decrease may be dependent on load.



Figure 4 shows the indent results for an uncoated glass and a  $\text{Si}_3\text{N}_4$ -coated glass sample. The measured fracture toughness of the coated glass is a strong function of load and therefore of sampled depth. In addition, the minimum load at which  $c = 2b$  is higher for the coated sample than for the uncoated sample. As was mentioned earlier, with coated glass and with some of the other substrates tested (except silicon), the threshold load required to produce any radial cracks is increased considerably. This indicates that the coatings inhibit crack initiation.

The surface fracture toughness was taken as the value of  $K$  at a fixed crack length,  $c'$ , from a least squares fit of  $K$  vs  $c^{1/2}$ . Values of  $c'$  were chosen to be as small as possible for each substrate in order to maximize the measured change in fracture toughness. The values of  $c'$  for glass and silicon substrates were  $60\text{ }\mu\text{m}$  and  $16\text{ }\mu\text{m}$ , respectively. Figures 5 and 6 show these surface fracture toughness values as a function of the square-root of the film thickness.

Several other substrates were tested with  $\text{Si}_3\text{N}_4$  and/or  $\text{Al}_2\text{O}_3$  coatings. Only a few samples were coated in these cases so the data should be considered less reliable. Table 1 gives the uncoated fracture toughness, the crack length at which the surface toughness was determined, and the increased fracture toughness extrapolated to a  $1.0\text{ }\mu\text{m}$  thick film using Eq. (2) (i.e., as  $d^{1/2}$ ). Also listed are the average grain sizes of the materials.

In most cases, the measured  $K_f$  is 2 to 6 times smaller than that predicted by Eq. (3). This is most likely caused by the presence of the tensile stress in the substrate or by the deviation from the penny-like shapes of the

cracks. Those sampled substrates with the smaller cracks tended to give larger changes. When the silicon and glass data are plotted versus  $c^{1/2}$  and extrapolated to zero crack length, the changes in toughness are approximately twice as high as those listed in Table 1.

Very high toughening was found for single crystal sapphire and no change was observed for fine grained  $\text{Si}_3\text{N}_4$  and  $\text{ZnS}$ . These anomalous results indicate that the toughening effect as measured by the Vickers indentation method may be dependent upon the mechanisms by which the surface stresses are accommodated in the substrate. The role of grain size and grain boundaries must be considered as must the levels of stresses in the bulk materials.

Complementary to this work, Burnett and Page<sup>8</sup> have made indent fracture measurements on ion-implanted sapphire. The implanted sapphire expands and produces a thin compressive layer near the surface. Using an implantation depth of  $0.2 \mu\text{m}$  for  $5.8 \times 10^{17} \text{ Y}^+$  ions/ $\text{cm}^2$  at 300 KeV and a stress of 5 GPa, the calculated  $K_f$  is 10 times larger than that measured using a 0.2 Kg load.

## CONCLUSIONS

Thin compressive films deposited onto brittle substrates are found to increase the measured indentation fracture toughness of a variety of materials. For a given substrate, the change in fracture toughness with respect to film stress, film thickness, and indent load can be modeled semi-quantitatively. Anomalously large increases are found for single crystal sapphire while no change is measured with polycrystalline  $\text{ZnS}$  or  $\text{Si}_3\text{N}_4$ .

## ACKNOWLEDGMENTS

The authors acknowledge David Marshall for helpful discussions and Kristin Wilson for help with the fracture toughness measurements. This work was supported in part by the Office of Naval Research under Contract N00014-85-C-0140, and by the Rockwell International Science Center Youth Motivation Program.

## REFERENCES

1. G.R. ANSTIS, P. CHANTIKUL, B.R. LAWN and D.B. MARSHALL, J. Am. Ceram. Soc. **64**, 533 (1981).
2. C.J. MCHARGUE, M.B. LEWIS, B.R. APPLETON, H. NARAWMOTO, C.W. WHITE and J.M. WILLIAMS, Proc. Int. Conf. on Science of Hard Materials, Jackson, Wyoming, August 23-28, 1981 (Plenum, 1983).
3. P.J. BURNETT and T.F. PAGE, J. Mat. Sci. **19**, 3524 (1984).
4. T. HIOKI, A. ITOH, M. OHKUBO, S. NODA, H. DOI, J. KAWAMOTO, and O. KAMAGAITO, J. Mat. Sci. **21**, 1321 (1986).
5. B.R. LAWN and E.R. FULLER, J. Mat. Sci. **19**, 4061 (1984).
6. P. CHAUDHARI, IBM J. Res. Develop. **13**, 197 (1969).
7. M. LAUGIER, J. Mat. Sci. **15**, 1147 (1980).
8. P.J. BURNETT and T.F. PAGE, J. Mat. Sci. **20**, 4624 (1985).

## FIGURE CAPTIONS

- Fig. 1 Stress distribution in a brittle material with a compressive surface film.
- Fig. 2 Schematic representation of a Vickers indent in a coated material.
- Fig. 3 Glass samples with a 1.0 kg load indent taken with an optical microscope. A) no film and B) with a  $0.4\text{ }\mu\text{m}$  thick  $\text{Si}_3\text{N}_4$  film. The arrows point to the ends of the surface radial cracks.
- Fig. 4 Measured fracture toughness of uncoated glass and glass coated with a  $0.7\text{ }\mu\text{m}$  layer of  $\text{Si}_3\text{N}_4$  as a function of indent load.
- Fig. 5 Surface fracture toughness of glass coated with  $\text{Si}_3\text{N}_4$ ,  $\text{SiO}_2$ , and  $\text{Al}_2\text{O}_3$  plotted as the  $1/2$  power of film thickness.
- Fig. 6 Fracture toughness of single crystal silicon coated with  $\text{Si}_3\text{N}_4$ ,  $\text{SiO}_2$  and  $\text{Al}_2\text{O}_3$  plotted as the  $1/2$  power of the film thickness.

Table 1  
Measured Fracture Toughness Data from Coated Ceramic and  
Single Crystal Substrates.

Substrate	Grain Size ( $\mu\text{m}$ )	$K_C$ ( $\text{MPam}^{1/2}$ )	$c'$ ( $\mu\text{m}$ )	Increase in Toughness $K_f$ ( $\text{MPam}^{1/2}$ ) 1 $\mu\text{m}$ Coating		
				$\text{Si}_3\text{N}_4$	$\text{SiO}_2$	$\text{Al}_2\text{O}_3$
ZnS	4	0.8	100	<0.1		<0.1
$\text{Si}_3\text{N}_4$	0.5	4.1	100	< 0.1		
Glass	Amorphous	0.62	60	0.5	0.3	0.17
Glass	Amorphous	0.62	60	(ZnS Coated)*		0.2
$\text{As}_2\text{S}_3$	Amorphous	0.16	50			0.10
Silicon	Single Xtal	0.74	16	0.7	0.4	0.3
Sapphire**	Single Xtal	1.7	16	1.7		1.5
ALON	75	1.43	16			0.5
Germanium	> 100	0.5	15	0.6		
Spinel	50	1.1	12			0.6
Calculated***				3.2	2.0	0.4

\*ZnS film deposited by laser evaporation and independently determined to have an intrinsic stress of 0.2 GPa

\*\* (0001) surface

\*\*\*Using Eq. (3).

SC36039

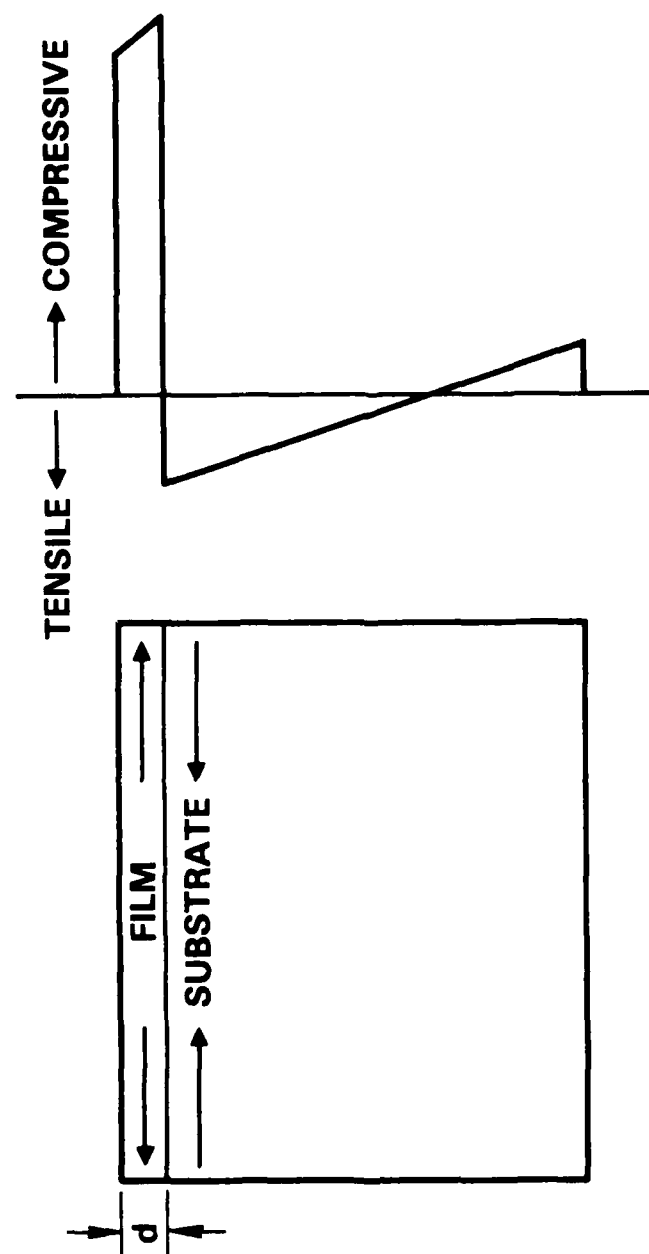


Fig. 1

SC38038

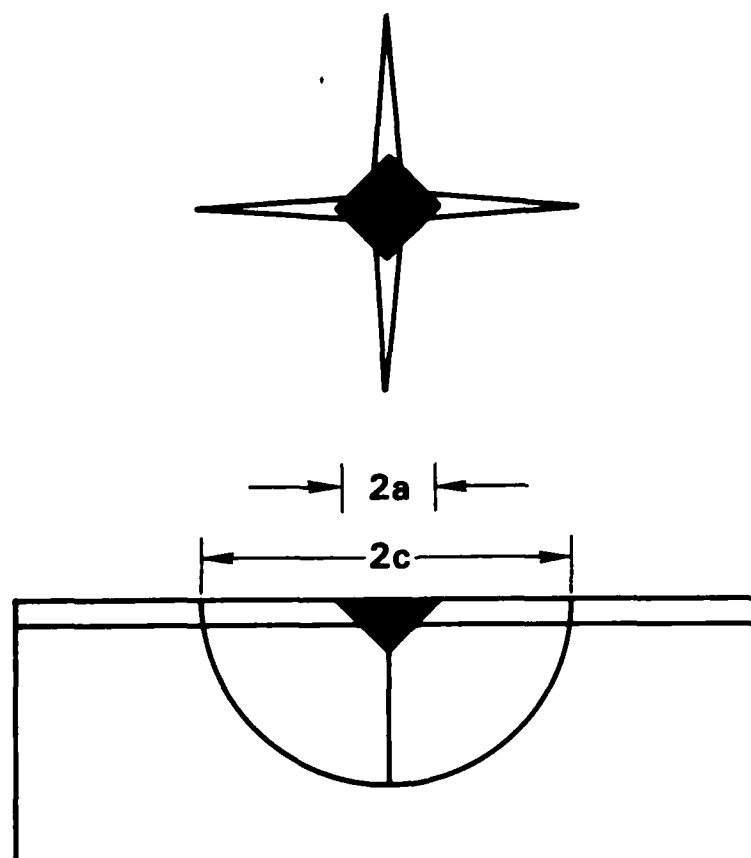


Fig. 2

SC39010



(b)



(a)

50 μm

Fig. 3



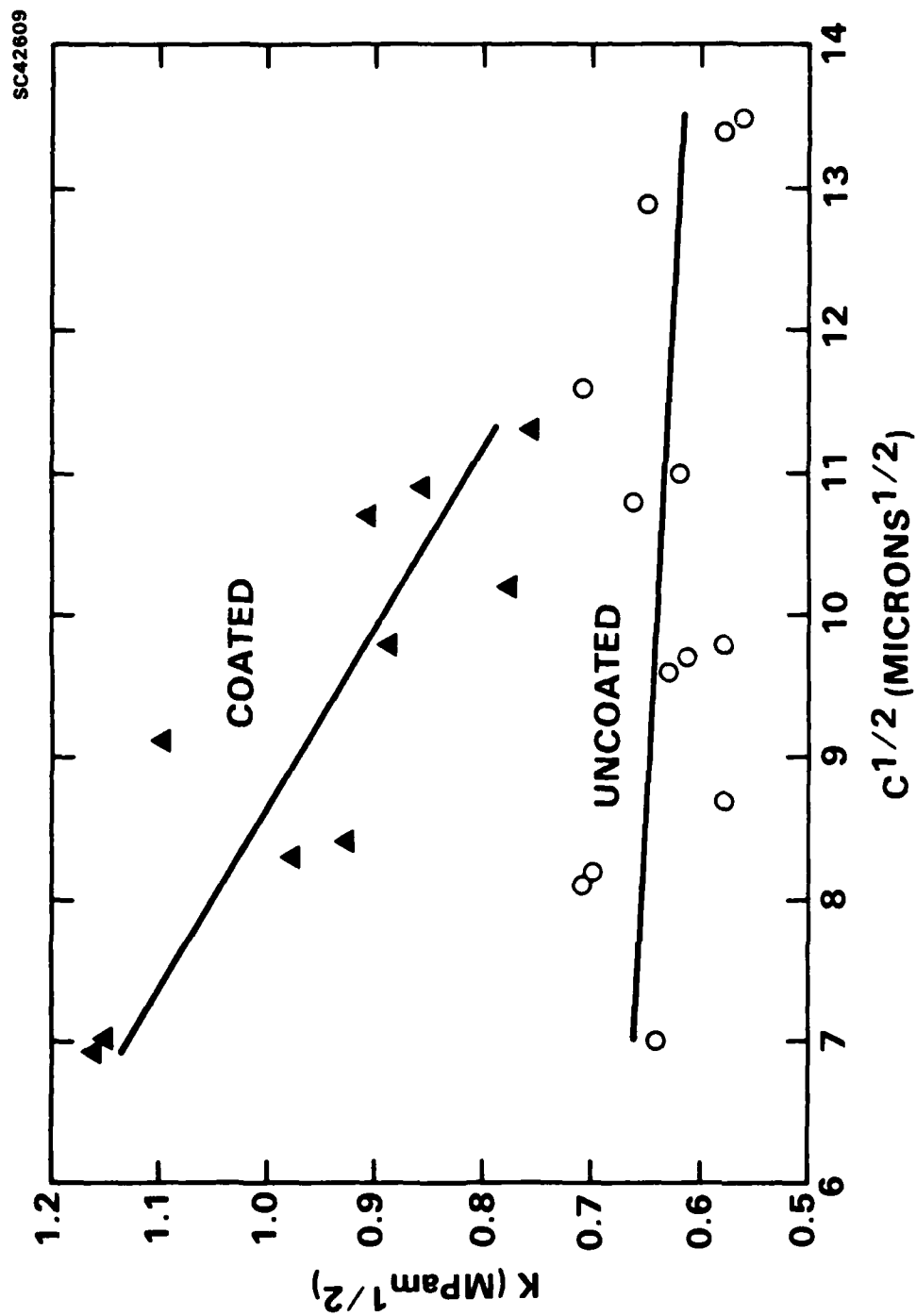


Fig. 4

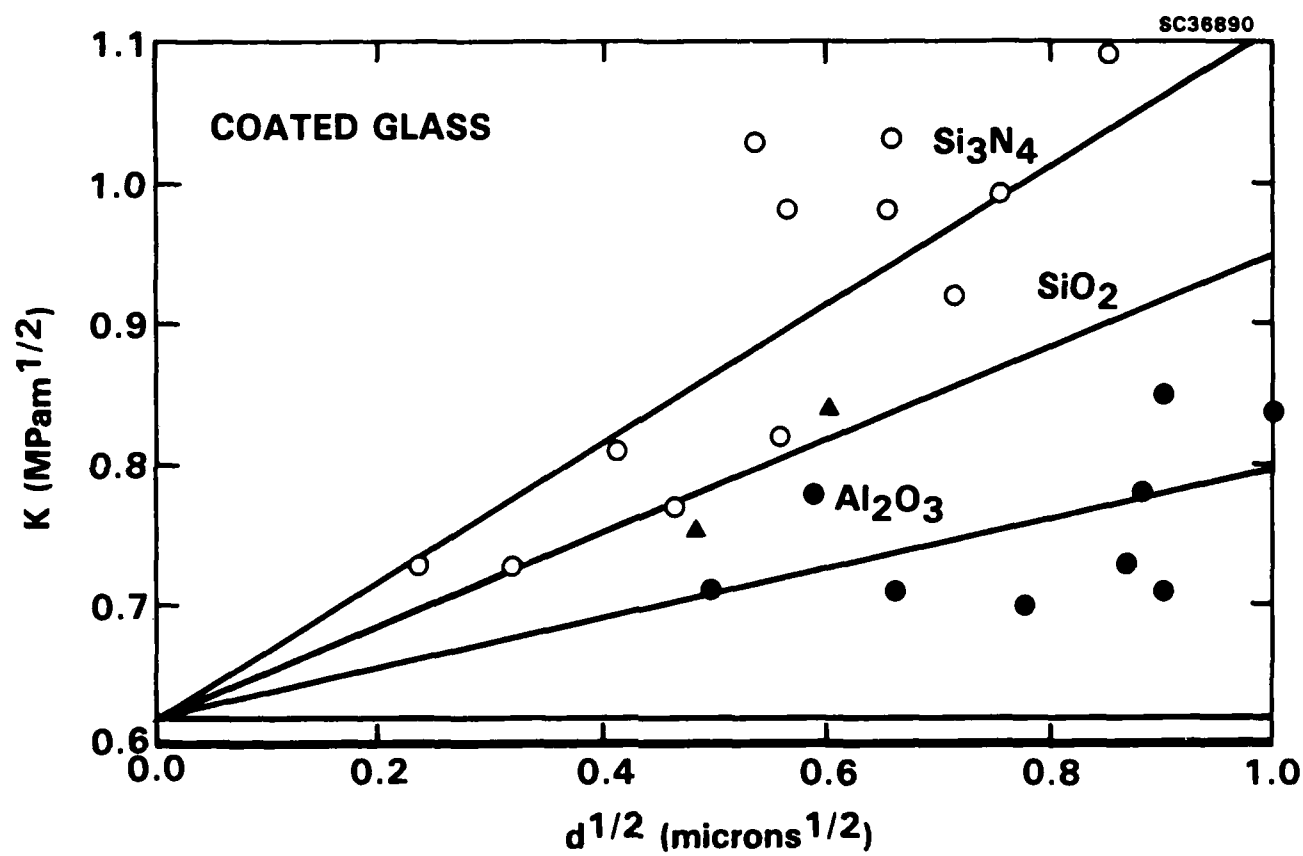


Fig. 5

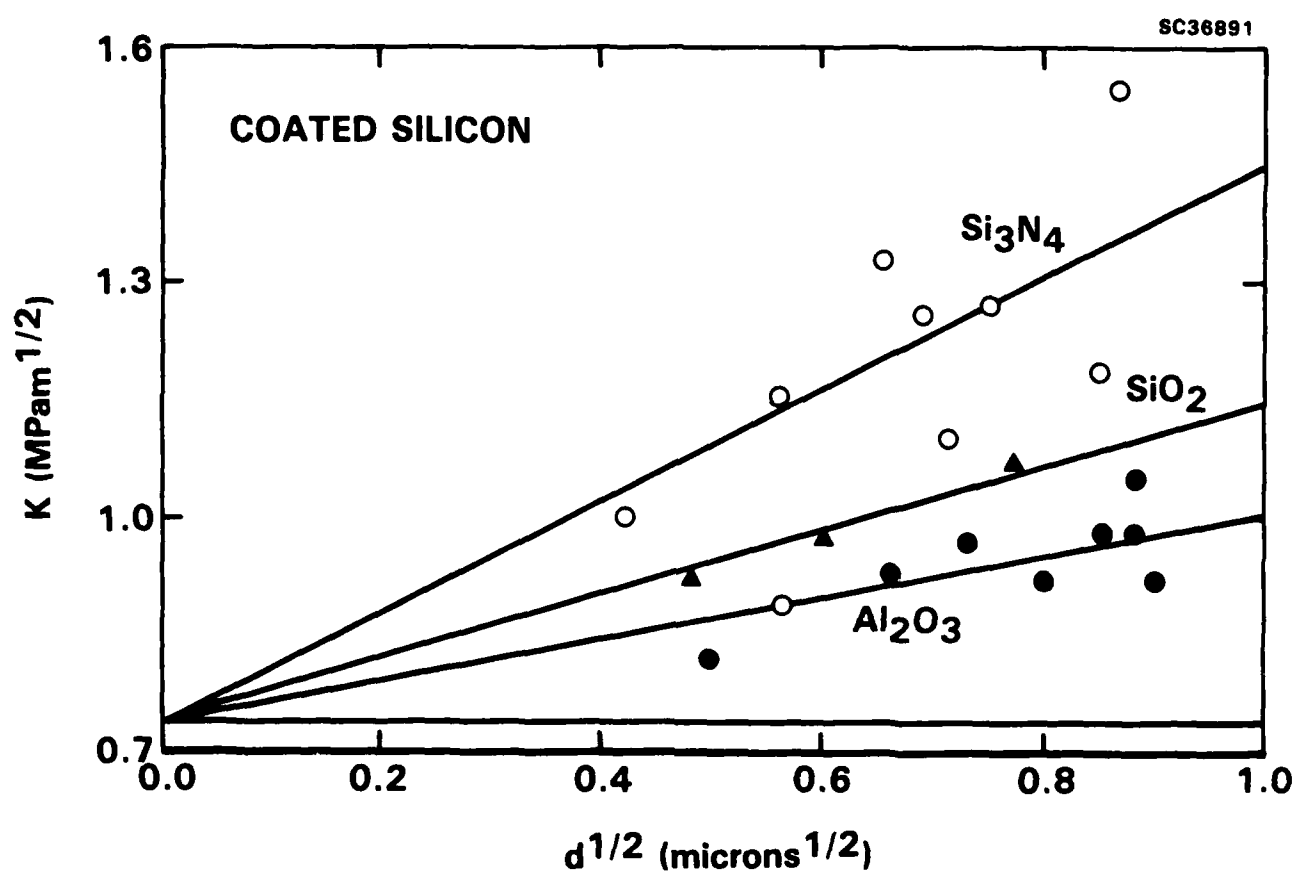


Fig. 6

END

DATE  
FILMED

6-1988

DTIC